SLAC-PUB-2460
January 1980
(T)

SURFACE PHYSICS AND THE ACCURACY OF LATTICE HAMILTONIAN TRUNCATION CALCULATIONS*

Moshe Aelion and M. Weinstein
Stanford Linear Accelerator Center
Stanford University, Stanford, California

ABSTRACT

We discuss the physical reason why keeping more states per site in a lattice truncation calculation gives more accuracy than keeping a small number of states and blocking more and more sites together in a given iteration. The specific example of the 1 + 1-dimensional Ising model in a transverse magnetic field is discussed in detail in order to show how attention paid to simple physics radically improves upon previous calculations.

Submitted to Physical Review D

---

* Work supported by the Department of Energy, Contract DE-AC03-76SF00515.

1. Introduction

The application of "real space renormalization group methods" to the study of lattice Hamiltonians has shown that one can learn quite a lot about the ground state and lowest lying states of a quantum system from an extremely crude approximation scheme.[1] It therefore becomes interesting to ask how hard it is to systematically improve the accuracy of these methods, and which schemes yield the greatest improvement for the least amount of work.

There have been several studies of this question within the context of simple models.[2] Most of these studies relate to the improvement one obtains by treating increasingly larger blocks exactly and holding the number of states per block, kept in any one truncation, to be equal to the number of states per site in the starting Hamiltonian. Unfortunately, the increase in accuracy obtained by these methods is not comparable to the increase in the difficulty of carrying them out. It is our purpose in this paper to point out that there are various ways in which one can rapidly improve accuracy for significantly less work, and to explain in simple physical terms why these methods work better than ones based on choosing larger and larger blocks as the basis of a truncation procedure.

2. The Free Field -- An Instructive Example

The method we will describe is an alternative truncation procedure which works with small blocks but keeps more states per block. There is a simple reason why this allows for greater improvement in accuracy; namely, properly implemented it reduces the "surface effects" coming from the fact that any single truncation is carried out in a block of

finite size. To see why this happens it is instructive to analyze the one-dimensional problem of a set of coupled harmonic oscillators. Let us begin by doing this within the framework of the more usual procedure and see how it can be greatly improved upon. To establish notation let us first consider a periodic Hamiltonian on a finite lattice, viz.

$$H = \sum_{j=-N}^{N} \left\{ \frac{p_j^2}{2} + \frac{\mu^2 x_j^2}{2} \right\} + \sum_{j=-N}^{N-1} \frac{1}{2}\left(x_{j+1} - x_j\right)^2 + \frac{1}{2}\left(x_N - x_{-N}\right)^2 \qquad (2.1)$$

This Hamiltonian is solved exactly by first defining

$$\begin{aligned} x_k &= \frac{1}{\sqrt{2N+1}} \sum_j e^{-ikj} x_j \quad , \\ p_k &= \frac{1}{\sqrt{2N+1}} \sum_j e^{-ikj} p_j \end{aligned} \qquad (2.2)$$

where the variable k refers to the discrete set of lattice momenta

$$k_p = 2\pi p/(2N+1) \qquad \text{for} \qquad -N \le p \le N \quad . \qquad (2.3)$$

With this notation we can rewrite H as

$$H = \sum_{k_p} \left[\frac{1}{2}\left(p_{-k_p} p_{k_p}\right) + \frac{\left(\mu^2 + 2(1 - \cos(k_p))\right)}{2} x_{-k_p} x_{k_p} \right] \qquad (2.4)$$

where p_k and x_k satisfy the commutation relations.

$$\left[p_{k'} , x_k \right] = -i\delta_{k',-k} \quad . \qquad (2.5)$$

In the usual way we introduce annihilation and creation operators

$$\begin{aligned} x_k &= \left(a_{-k} + a_k^+ \right) / \sqrt{2\omega_k} \\ ip_k &= \left(a_{-k} - a_k^+ \right) / \sqrt{\omega_k/2} \end{aligned}$$

where

$$\omega_k \equiv \sqrt{2(1-\cos(k))+\mu^2}$$

and (2.6)

$$\left[a_k, a_{k'}^{+}\right] = \delta_{k,k'} \quad ,$$

and rewrite H as

$$H = \sum_k \omega_k \left(a_k^{+} a_k + 1/2\right) \tag{2.7}$$

In the infinite volume limit

$$\frac{1}{(2N+1)} \sum_k \rightarrow \frac{1}{2\pi} \int_{-\pi}^{\pi} dk$$

and H becomes

$$H = \frac{L}{2\pi} \int_{-\pi}^{\pi} \omega_k \left(a_k^{+} a_k + 1/2\right) \quad . \tag{2.8}$$

So much for the exact solution. Let us now see how a naive truncation calculation of an approximate ground state of the infinite volume theory procedes. To begin we divide the infinite lattice into blocks of size $L_B = (2N_B + 1)$ and rewrite H as

$$H = \sum_{s=-\infty}^{\infty} \sum_{r=-N_B}^{N_B} \left(\frac{p^2_{L_B s+r}}{2} + \frac{(\mu^2+2)}{2} x^2_{L_B s+r} - x_{L_B s+r}\, x_{L_B s+r+1} \right) \tag{2.9}$$

Next comes the truncation step. This amounts to reducing the L_B degrees of freedom per block to a single degree of freedom. To be precise let us define this procedure by first introducing variables $X_s(K)$, $P_s(K)$ where

$$X_s(K) = \frac{1}{\sqrt{L_B}} \sum_{r=-N_B}^{N_B} e^{-iKr} X_{L_B s+r}$$

$$P_s(K) = \frac{1}{\sqrt{L_B}} \sum_{r=-N_B}^{N_B} e^{-iKr} P_{L_B s+r}$$

and where

$$K = 2\pi \ell / L_B \quad , \quad -N_B \leq \ell \leq N_B \quad ; \tag{2.10}$$

we then freeze out all but the $K = 0$ degrees of freedom. This is most simply carried out if we rewrite H by adding and subtracting the terms $\sum_s X_{L_B s+N_B} X_{L_B s-N_B}$ and substituting (2.10) into the resulting expression. We thus obtain

$$H = H_0 + V$$

where

$$H_0 = \sum_{K,s} \left[\frac{1}{2} P_s(-K) P_s(K) + \frac{\left(\mu^2 + 2(1 - \cos(K)) + 2/L_B\right)}{2} X_s(-K) X_s(K) \right]$$

and

$$V = \sum_{\substack{K \neq K' \\ s}} \frac{e^{i(K-K')N_B}}{L_B} X_s(K) X_s(K') - \sum_{s,K,K'} \frac{e^{i(K-K')N_B}}{L_B} X_s(K) X_{s+1}(K') \tag{2.11}$$

Introducing annihilation and creation operators as in Eq. (2.6) with

$$\omega_K \equiv \sqrt{\mu^2 + 2(1 - \cos(K)) + 2/L_B}$$

we can diagonalize H_0. The naive truncation procedure is to eliminate all but the degrees of freedom X_s $(K = 0)$. This is accomplished by restricting the class of trial states to those[14] which satisfy the condition $a_s(K)|\psi\rangle = 0$ for all $K \neq 0$. Under this assumption if $|\psi\rangle$ and

$|\varphi\rangle$ are two such states, then

$$\langle\varphi \mid H_0+V \mid \psi\rangle = \sum_s \left\{ \sum_{K\neq 0} \frac{1}{2}\sqrt{\mu^2 + 2(1-\cos(K)) + 2/L_B} \right\} \langle\varphi|\psi\rangle$$

$$+ \langle\varphi \mid \sum_s \left\{ \frac{1}{2} P_s(K=0)^2 + \frac{1}{2}(\mu^2 + 2/L_B) X_s(K=0)^2 \right.$$

$$\left. - \frac{1}{L_B} X_s(K=0)\ X_{s+1}(K=0) \right\} |\psi\rangle$$

$$\equiv \langle\varphi \mid H_1^{eff} \mid \psi\rangle \qquad (2.12)$$

where, $|\psi\rangle$ and $|\varphi\rangle$ are arbitrary square integrable functions of the variables $X_s(K=0)$. Having arrived at (2.12) we drop the label $K=0$ from our notation for the operator $X_s(K=0)$ and observe that we can obtain an upper bound on the ground state energy of the theory by diagonalizing the effective Hamiltonian

$$H_1^{eff} = (Vol)\,\varepsilon_0 \mathbb{1} + \sum_s \left\{ \frac{1}{2}P_s^2 + \frac{(\mu^2 + 2/L_B)}{2} X_s^2 - \frac{1}{L_B} X_s X_{s+1} \right\} \qquad (2.13)$$

where $\mathbb{1}$ is the identity operator,

$$\varepsilon_0 \equiv \frac{1}{L_B} \sum_p \left\{ \frac{1}{2}\sqrt{\mu^2 + 2(1-\cos(2\pi p/L_B)) + 2/L_B} \right\} \qquad (2.14)$$

and P_s and X_s satisfy canonical commutation relations (2.10). Obviously H_1 could be as easily diagonalized as H and one would obtain an upper bound on the ground state energy density, which for the infinite volume case is

$$\varepsilon_1 = \varepsilon_0 + \frac{1}{2\pi L_B} \int_{-\pi}^{\pi} \frac{dk}{2} \sqrt{\mu^2 + 2(1-\cos(K))/L_B} \qquad (2.15)$$

In fact, this is not a bad bound on the true ground state energy density even for $L_B = 3$. Even if one pretends one does not know how to diagonalize (2.13) and instead iteratively carries out the same procedure one obtains a reasonable bound of the form

$$\varepsilon_{var} = \lim_{M \to \infty} \sum_{\ell=1}^{M} \left[\frac{1}{(L_B)^{\ell}} \varepsilon_{\ell} \right] \tag{2.16}$$

where

$$\varepsilon_{\ell} \equiv \sum_{p=-N}^{N} \frac{1}{2} \sqrt{\mu^2 + 2\left[(1 - \cos(2\pi p/L_B)) + 1\right]/L_B^{\ell}} \tag{2.17}$$

If the only quantity of interest was the ground state energy density, this would be an entirely satisfactory state of affairs. However, one would like to use this method to learn something about the spectrum of low lying states and the behavior of correlation functions. For these purposes, one needs to do well in computing not only the energies of states at zero momentum, but also the way in which these states condense down on zero; i.e., one needs to compute the density of states near $K = 0$. Examination of (2.17) for the massless limit, $\mu^2 = 0$, shows that the naive truncation procedure doesn't do so well in this regard. The point is that, as can be seen from (2.17), after ℓ-iterations the $p = 0$ mode has a frequency $W_0(\ell)$ given by $(2/L_B)^{\ell/2}$. This means that states are condensing down onto the true $K = 0$ mode as the square root of $1/L_B^{\ell}$ - which is the length of the block under consideration. Of course, for the true free field case, Eq. (2.4), on a block of length $(L_B)^{\ell}$ with periodic boundary conditions, we see that for $\mu^2 = 0$, W_0 for the $K = 0$ mode vanishes and the neighboring modes are spaced from it by an amount

$1/L_B^{\ell}$. The common factor of $(1/L_B)^{\ell/2}$ in all energies is a surface effect due to truncating on finite size sub-blocks and survives only because of the prescription we have adopted of truncating to a single mode per box. Having made this observation the cure is apparent. Simply truncate to more than one mode per box. For example, suppose in the first step we keep the lowest three oscillator modes per box of length L_B. Our effective truncated Hamiltonian will then describe a lattice system of three harmonic oscillators per site 'j', i.e., x(j), y(j), and z(j), and will have the form.

$$
\begin{aligned}
H^{eff} = \sum_j \; & \frac{1}{2}\left(P_x(j),\, P_y(j),\, P_z(j)\right)\begin{pmatrix} 1 & 0 & 0 \\ 0 & 1 & 0 \\ 0 & 0 & 1 \end{pmatrix}\begin{pmatrix} P_x(j) \\ P_y(j) \\ P_z(j) \end{pmatrix} \\
& + \frac{1}{2}\left(x(j),\, y(j),\, z(j)\right)\begin{pmatrix} \omega_x^2 & 0 & 0 \\ 0 & \omega_y^2 & 0 \\ 0 & 0 & \omega_z^2 \end{pmatrix}\begin{pmatrix} x(j) \\ y(j) \\ z(j) \end{pmatrix} \\
& - \frac{1}{L_B}\left(x(j),\, y(j),\, z(j)\right)\begin{pmatrix} K_{11} & K_{12} & K_{13} \\ K_{21} & K_{22} & K_{23} \\ K_{31} & K_{32} & K_{33} \end{pmatrix}\begin{pmatrix} x(j+1) \\ y(j+1) \\ z(j+1) \end{pmatrix}
\end{aligned}
\tag{2.18}
$$

where the K_{ij}'s are numbers whose modulus is of order unity, and ω_x^2, ω_y^2, and ω_z^2 are all of order $2/L_B$ and differ by terms of order $1/L_B^2$. Clearly, in the next iteration remixing of these terms will produce

oscillators having frequencies, which are in fact split from the lowest one, by order $1/L_B^2$. Thus, freezing out all but the three lowest modes does produce a reasonable representation of the density of states factor for the $\mu^2 = 0$ case, As in example of this effect and the importance of keeping more oscillators per block see Ref. 3.

The moral to be drawn from this discussion of the free field is, as we said at the outset, that in order to minimize "surface effects" arising from the truncation algorithm it is more important to keep additional degrees of freedom (i.e., for finite spin systems--more states) than it is to work with larger and larger blocks. In the next section we will show how well an algorithm based upon this observation works for the simple case of the 1+1 dimensional Ising model in a transverse magnetic field.

3. Analysis of the Ising Model in a Transverse Field

The theory to be discussed in this section is a one space-one time theory of elementary spins on a line, having a Hamiltonian.

$$H = \sum_j \left[\frac{\varepsilon_o}{2} \sigma_z(j) - \Delta_o \sigma_x(j)\sigma_x(j+1) \right] \tag{3.1}$$

A simple-minded analysis of this system was described in Ref. 4, and a more complex variational method for improving upon these results within the restriction of keeping at each step only two states per block was presented. Typical results obtained for these calculations are given in Table 1 compared to results for the more complex calculations to be described in this section. These calculations all involve keeping more

states per block, but the very best of the calculational schemes uses the previous "two level variational renormalization group" results as input to a multistate calculation. In order to make the details of this calculational scheme clear we briefly remind the reader of the principles of the two state truncation calculation. (See Ref. 4 for a detailed discussion.)

A. Variational Renormalization Group Analysis of Ising Model

The basic procedure followed in analyzing H as defined in (3.1) is to block the lattice into pairs of sites, i.e., define $j = 2_p + r$, $r = 0,1$. One then thins the number of states to be used in our trial wave function for the ground state. To accomplish this we define $|\uparrow_j\rangle$ and $|\downarrow_j\rangle$ to be eigenstates of $\sigma_3(j)$ with eigenvalues ± 1. We then note that a basis for the full Hilbert space of the theory is generated by taking tensor products over all sites 'j' of these 2 states per site; hence, for a lattice of length L we have a 2^L dimensional space of states. We next construct, using these states, a subspace having half as many states. To do this we define two states, associated with each block 'p'.

$$|\downarrow'_p\rangle \equiv \frac{1}{\sqrt{1 + a^2(\varepsilon_o/\Delta_1)}} \left(|\downarrow_{2p+1}\rangle + a(\varepsilon_o/\Delta_o)\ |\uparrow_{2p}\uparrow_{2p+1}\rangle \right)$$

and

$$|\uparrow'_p\rangle \equiv \frac{1}{\sqrt{2}} \left(|\uparrow_{2p}\downarrow_{p+1}\rangle + |\downarrow_{2p}\uparrow_{2p+1}\rangle \right) \qquad (3.2)$$

and then forming the $2^{L/2}$ states which can be made by taking arbitrary tensor products of these two states per block. The next step is to compute matrix elements of H between arbitrary states of this type. In this way one obtains a truncated or effective Hamiltonian of the form

$$H_1^{eff} = \sum_p \left[C_1 \mathbb{1}_p + \frac{\varepsilon_1}{2} \sigma_z(p) - \Delta_1 \sigma_x(p)\sigma_x(p+1) \right] \tag{3.3}$$

where, by definition

$$\sigma_z(p)|\uparrow_p'\rangle \equiv |\uparrow_p'\rangle \quad ,$$

$$\sigma_z(p)|\downarrow_p'\rangle \equiv -|\downarrow_p'\rangle \quad ,$$

and

$$\sigma_x(p)|\uparrow_p\rangle = |\downarrow_p\rangle \quad ,$$

$$\sigma_x(p)|\downarrow_p\rangle = |\uparrow_p\rangle \quad , \tag{3.4}$$

and where C_1, ε_1 and Δ_1 are given in terms of ε_0, Δ_0 and $a(\varepsilon_0/\Delta_0)$ by the equations.

$$\varepsilon_1 \equiv \varepsilon_0(1 - a_0^2) - \Delta_0(1 - a_0)^2 \,/\, (1 + a_0^2)$$

$$\Delta_1 \equiv \frac{\Delta_0(1 + a_0)^2}{2(1 + a_0^2)}$$

$$C_1 = 2\,C_o - \left[\frac{\varepsilon_0(1 - a_0^2) + \Delta_0(1 + a_0)^2}{2(1 + a_0^2)} \right] \tag{3.5}$$

and $a_0 \equiv a(\varepsilon_0/\Delta_0)$ is for the moment an undefined function of $y_0 = (\varepsilon_0/\Delta_0)$. Clearly, the lowest eigenvalue of H_1^{eff} is an upper bound on the lowest eigenvalue of H in (3.1). This procedure is carried out iteratively until ε_n or Δ_n becomes sufficiently small that the Hamiltonian, H_n^{eff}, can be exactly diagonalized or well treated perturbatively. The best "two level" truncation scheme calculation is based upon the observation that we get a different renormalization group prescription for each choice of the function a(y). Hence, we can choose some parametrization for an arbitrary function of this form, compute the bound on the ground state energy density obtained for a given choice of parameters--where this bound is nothing but to

$$\mathcal{E}\Big(a(y)\Big) \equiv \lim \left(\frac{1}{2^n} C_n\right) \tag{3.6}$$

and then vary the parameters defining a(y) so as to obtain the best bound. The explicit form of a(y) used to obtain the results in Table 1 was

$$\tan^{-1}\Big(a(y)\Big) \equiv \frac{\pi}{4}\left[\frac{1 - \tanh(\alpha y - \beta)}{1 - \tanh(-\beta)}\right] \tag{3.7}$$

where α, β were the two variational parameters.

B. The Multistate Calculations: Naive Truncation Scheme

With the discussion of Section 3A behind us it is simple to define the general multistate calculation. It proceeds in a similar fashion. First one blocks the lattice into units of length L_0 by letting

$j = L_o p + r$, $r = 0, \ldots, L_o - 1$. In general there are 2^{Lo} states associated with each block and a basis for the full Hilbert space of the theory is obtained by taking tensor products of these individual block states. The first step of the calculation is to choose some number, say M, states out of these 2^{Lo} states and compute H_1^{eff}. This leads to a Hamiltonian of the form

$$H_1^{eff} = \sum_p \left[C_1 \mathbb{1}_p + C_2 \mathcal{H}_{ss}(p) + S_x^R(p) S_x^L(p+1) \right] \tag{3.8}$$

where $\mathbb{1}_p$, $\mathcal{H}_{ss}(p)$, $S_x^R(p)$ and $S_x^L(p)$ are M x M matrices. The columns in Table 1 labeled "naive truncation calculation" are produced by pairing sites, i.e., letting $p = 2\ell + r$, $r = 0, 1$, choosing for block 'ℓ'--the lowest M eigenvectors of

$$\mathcal{H}(\ell) = \left\{ C_2 \left(\mathcal{H}_{ss}(2\ell) + \mathcal{H}_{ss}(2\ell + 1) \right) - S_x^R(2\ell) S_x^L(2\ell + 1) \right\} \tag{3.9}$$

out of the M^2 eigenvectors in this block, and truncating $\mathcal{H}_1^{eff}$ to the subspace spanned by tensor products over these states. Evidently, this sort of calculation is carried out by means of a computer and, referring to the Table I and II we see that keeping eight states per block results in considerable improvement in accuracy over the two site "variational renormalization group equation." However, one can do still better by folding the 2 state variational renormalization calculation results into the multi-state calculation and the results in the last three columns of Tables I and II and in all of the other Tables and Figs. 3-11 show the results of the calculational scheme, to be described in Section 3C.

C. Multistate Calculation — A Hybrid Technique

The calculations to be described in this section allow us to combine the best attributes of the preceding set of calculations with no appreciable increase in labor. It does not take much thought to realize that this is a desirable thing to do since on the one hand the multistate calculation is myopic, in that it treats the physics of short distances very well but does not allow a great deal of feedback of effects that are important for a very large number of sites into the short distance calculation; and, on the other hand the two level variational renormalization group scheme sacrifices accuracy in the treatment of short distance effects in order to maximize the effects of long distance physics. Clearly, the two calculations provide complementary information.

Before going on to describe the hybrid calculation it is worth pointing out that the intuitive notion that the naive multistate calculation and two level variational renormalization group calculation provide complementary information can be reasonably well quantified. This is because the theory specified in (3.1) can be transformed to an equivalent spin 1/2 theory for which the roles of ε_o and Δ_o are interchanged. This is the familiar duality transformation in which one defines new spin operators

$$S_x(j) = \prod_{i=-\infty}^{j-1} (-1)^i \sigma_x(i)$$

$$S_z(j) = -\sigma_x(j-1)\,\sigma_x(j) \tag{3.10}$$

and rewrites H as

$$H = \Delta_o \sum_j \left\{ \frac{y_o}{2}\sigma_z(j) - \sigma_x(j)\,\sigma_x(j+1) \right\} = \frac{\Delta_o y_o}{2} \sum_j \left\{ \frac{2}{y_o} S_B(j) S_x(j+1) \right\} \tag{3.11}$$

where

$$y_o = \varepsilon_o/\Delta_o$$

It is clear that the ground state energy of either the Hamiltonian depends only, up to an overall scale factor, on the coefficient of the $\sigma_z(j)$ term; it follows that,

$$E_o(y_o) = \frac{y_o}{2} E_p(4/y_o) \tag{3.12}$$

This formula is satisfied by the exact solutions for $E_o(y)$ and in general is poorly satisfied by simple approximation procedures. In Fig. 1 the solid curve is the plot of the exact ground state energy as a function of y_o and the dashed curve is a plot of the two level variational renormalization group calculation of this quantity. It is clear that this calculation is better for the region $y < 2$ than for $y > 2$. In Fig. 2 we see a comparison of the results of a naive 8-level truncation calculation with the curve which would be obtained using Eq. (3.12) to reflect

results of the two level calculation for $y < 2$ to $y > 2$. As is clear from Fig. 2 the 8-level calculation for $y > 2$ very nearly approximates the results obtained by dualizing the results of the variational two level calculation for $y < 2$. Since the duality transformation (3.10) interchanges order and disorder variables--or short range and long range information--we see in highly graphic form that the two types of approximation procedures provide complementary information. The next problem is to combine them so as to get the benefit of both types of information.

This is easily accomplished. In the tables and pictures to follow the explicit results we present were obtained from a straightforward procedure which began by combining sets of four sites into a single block and keeping only a set of 6, 7, or 10 states out of the 16 possible states per block in order to initialize our multistate Hamiltonian. The particular 6, 8, or 10 states were chosen according to an algorithm which differed in our important way from the naive truncation algorithm: namely, if we decided to keep 2N states, then only the first 2 (N-1) of these states were chosen to be the lowest eigenstates of the block Hamiltonian. The remaining two states are chosen so that one can,by forming linear combinations of the 2N states, generate the states $|\uparrow'\rangle$ and $|\downarrow'\rangle$ which one would have generated after two iterations of Eq. (3.2) and (3.5) and using the form of a(y) given in (3.7). To be precise, one first forms the states (for block 'p')

$$|\psi'_p\rangle = \frac{1}{\sqrt{1+a_1^2}}\left\{\left(\frac{|\downarrow\downarrow\downarrow\downarrow\rangle + a_o|\downarrow\downarrow\downarrow\uparrow\rangle + a_o|\uparrow\downarrow\downarrow\downarrow\rangle + a_o^2|\uparrow\downarrow\downarrow\uparrow\rangle}{\left(1+a_o^2\right)}\right)\right.$$

$$\left. + \frac{a_1}{2}\left(|\downarrow\uparrow\downarrow\uparrow\rangle + |\downarrow\uparrow\uparrow\downarrow\rangle + |\uparrow\downarrow\downarrow\uparrow\rangle + |\uparrow\downarrow\uparrow\downarrow\rangle + a_o|\uparrow\downarrow\uparrow\uparrow\rangle\right)\right\}$$

$$|\uparrow'_p\rangle = \frac{1}{2(1+a_o^2)}\left(|\downarrow\uparrow\downarrow\uparrow\rangle + |\downarrow\uparrow\uparrow\downarrow\rangle + a_o|\uparrow\downarrow\uparrow\uparrow\rangle\right) \qquad (3.13)$$

where

$$a_o = a(\varepsilon_o/\Delta_o) \quad ; \quad a_1 = a(\varepsilon_1/\Delta_1)$$

and ε_1 and Δ_1 are given in terms of ε_o and Δ_o by Eq. (3.5); one then Gram-Schmidt orthonormalizes the set of 2N states obtained by adjoining the states in (3.13) to the set of 2 (N - 1) lowest (four even and odd) eigenstates of the Hamiltonion for block 'p'. This set of states has the virtue that it contains all the information carried in an iterative 2(N - 1) naive truncation procedure and also one has kept all the states needed to construct the two level variational wave functions at the next step of the calculation. The iteration procedure is to block this effective lattice theory having 2N-states per site into block of 2-sites or $4N^2$ states, i.e., let p = 2r + s, s = 0,1, and diagonalize the resulting $4N^2 \times 4N^2$ matrix. One then truncates the $4N^2$ states to 2(N - 1) states ((N - 1) - even and (N - 1) - odd levels) and then one once again adjoins the states needed to span the vectors

$$|\downarrow'_r\rangle = \frac{1}{\sqrt{1 + a_2^2}} \left(|\downarrow'_{2r} \downarrow'_{2r+1}\rangle + a_2 |\uparrow'_{2r} \uparrow'_{2r+1}\rangle \right)$$

$$|\uparrow'_r\rangle = \frac{1}{\sqrt{2}} \left(|\downarrow'_{2r} \uparrow'_{2r+1}\rangle + |\uparrow'_{2r} \downarrow'_{2r+1}\rangle \right) \tag{3.14}$$

where

$$a_2 = a(\varepsilon_2/\Delta_2)$$

and ε_2 and Δ_2 are defined in terms of a_1, ε_1, and Δ_1 by the obvious generalizations of (3.5). Since, at each stage we are carrying along the ability to reconstruct the two level variational groundstate wavefunctions, this procedure guarantees that we will get a groundstate energy that is lower than either the $2(N-1)$ naive truncation answer or the two level-variational calculation. Moreover, considering the results shown in Figs. 1 and 2, the answers should be considerably better in terms of self duality. This is in fact borne out in the calculations which have been carried out for the cases $2N = 6$, 8, and 10--and the results are shown in the tables and figures which follow.

4. Discussion of Results

There is not much that needs to be said about the tables and figures that follow; they essentially speak for themselves. The purpose of Figs. 3 - 11 is to show how good the analysis of the model is for all values of $y \equiv \varepsilon/\Delta$ when one keeps 10 states at each iteration. Figures 12 and 13 are included to give a feeling for how the accuracy changes as one adds additional states. In all figures the plotted points represent

the results of independent calculations done by means of the same algorithm for each value of 'y_0'. This is important since none of these calculations are based upon an extrapolation of a perturbation expansion, and--at least to our minds--it is astonishing how accurate such an apparently crude approximate scheme can be made. The solid curve in Fig. 3 gives the result of the exact calculation of the ground state energy density. The same information is obtainable from Table I where one can also see what kind of increases in accuracy result from adding 2 states at a time. The solid curve in Fig. 4 is a plot, not of the exact magnetization, i.e., $\frac{1}{V} \sum_j \langle \sigma_z(j) \rangle$ as a function of 'y', but rather it is a plot of the functional form of the exact answer.

$$\frac{1}{V} \sum \langle \sigma_x(y) \rangle = \left(1 - (y/y_c)^2\right)^{1/8} \qquad (4.1)$$

for the calculated value of $y_c = 2.08$ instead of the exact value which is $y_c = 2$. The fit is remarkably good, except for the error in the critical point. Perhaps one of the most striking curves is Fig. 5 which is $\partial^2 E_g / \partial y^2$. Once again the solid curve is the exact answer plotted for the wrong value of y_c, i.e., 2.08 instead of 2. Apparently, the point by point calculation has no trouble reproducing a reasonable fit for the true logarithmic singularity over a large range of coupling constant. This result is the first indication that the scheme is doing more than producing a good value for the ground state energy density, since this quantity requires a reasonably correct treatment of the density of states factors. The next three curves provide further support

for this picture in that they compare the exact ($y_c = 2$) calculations or the nearest neighbor correlation functions

$$\frac{1}{V} \sum_{\partial} \langle \sigma_x(j)\sigma_x(j+1) \rangle \quad , \quad \frac{1}{V} \sum_{\partial} \langle \sigma_y(j)\sigma_y(j+1) \rangle$$

and

$$\frac{1}{V} \sum_{\partial} \langle \sigma_z(j)\sigma_z(j+1) \rangle$$

against the approximate calculations. Once again, the agreement is surprisingly good given the crude nature of the calculation scheme; and once again, these quantities are related to getting more than the ground state energy correctly. As a further test of this question one compares the direct computations of the mass gap of the theory above $y_c = 2$ with the exact prediction; here one sees that one does quite well except in the vicinity of the critical point. Figure 11 dramatically shows that keeping more states is most important in doing well in this quantity and therefore pinning down the exact location of the critical point. From Fig. 10 we see that although keeping more states only modestly improves the ground state energy, even two extra states pay large dividends in computations of the mass gap. The tables allow one to get a more quantitative feel for the results summarized in the various figures.

Conclusions

We feel that these calculations show that the small errors in the properties of ground state wave function which make the variational two-level truncation scheme inaccurate are probably correctly identified as due to the effective "surface terms" introduced by the truncation procedure. Moreover it is clear that the strategy suggested by the example of the free field, namely keeping more degrees of freedom per block, rapidly pays off in significant improvements in accuracy. Nevertheless, we are surprised by how well the crude calculational scheme of this type can do, and it would be very interesting if further studies of this sort could provide a firmer understanding of why it works so well. Even in the absence of this information it is clear that the scheme can provide the basis of a systematically improvable method for analyzing the properties of quantum lattice theories.

REFERENCES

1. S. D. Drell, M. Weinstein, and S. Yankielowicz, Phys. Rev. D 16, 1769 (1977); R. Julien, J. Fields, and S. Doniach, Phys. Rev. Lett. 38, 1500 (1977); S. D. Drell, B. Svetitsky, M. Weinstein, Phys. Rev. D 17, 523 (1978); S. D. Drell and M. Weinstein, Phys. Rev. D 17, 3203 (1978); R. Julien, J. N. Fields, and S. Doniach, Phys. Rev. B 16, 4889 (1977); R. Julien, P.Pfeuty, J. N. Fields, and S. Doniach, Phys. Rev. B 18, 3568 (1978), K. Uzelac, P. Pfeutry, and R. Julien, Phys. Rev. Lett. 43, 805 (1979); S. D. Drell, H. Quinn, B. Svetitsky, and M. Weinstein, Phys. Rev. D 19, 619 (1979); J. M. Rabin, SLAC-PUB-2391, Sept. 1979 (submitted to Phys. Rev.); K. Zuelac, R. Julien, and P. Pfenty, preprint from Laboratoire de Physique des Solides, Université de Paris-Sud, Centre d'Orsay.

2. R. Julien, J. N. Fields, and S. Doniach, Phys. Rev. B 18, 3568 (1978).

3. S. D. Drell and M. Weinstein, Phys. Rev. D 17, 3202 (1978).

4. S. D. Drell, M. Weinstein, and S. Yankielowicz, Phys. Rev. D 16, 1769 (1977).

Table I

GROUND STATE ENERGY DENSITY FOR VARIOUS VALUES OF $y = \epsilon/\Delta$, CALCULATED BY DIFFERENT METHODS

Energy Density	Exact Solution	2 Site Simple Truncation	2 Site Variational	8 State Simple Truncation	H 6	H 8	H 10
0	-1	-1	-1	-1	-1	-1	-1
.4	-1.010025	-1.0028	-1.010012	-1.00817	-1.0100	-1.0100125	-1.0100187
.8	-1.040417	-1.01562	-1.040197	-1.03391	-1.0401984	-1.04020200	-1.040196
1.	-1.063544	-1.03153	-1.062978	-1.05406	--	-1.0629915	--
1.8	-1.216001	-1.16934	-1.207562	-1.1952	-1.20816	-1.20818	-1.2081956
2.	-1.27324	-1.22402	-1.257837	-1.25166	-1.25913	-1.259868419	-1.260134
2.2	-1.342864	-1.2872	-1.131425	-1.32314	-1.31839	-1.32030	-1.32555838
3.	-1.671926	-1.61484	-1.61612	-1.65648	--	--	--
3.2	-1.760508	-1.70581	-1.70667	-1.84584	-1.74101	-1.741507	-1.747104
4.	-2.127089	-2.08095	-2.081156	-2.11487	-2.11118	-2.111389	-2.1161878

Table II

MAGNETIZATION, $\frac{1}{V}\sum_j \langle\sigma_x(j)\rangle$, FOR THE SAME VALUES OF y CALCULATED BY SEVERAL METHODS

y	Exact Solution	2 Site Simple Truncation	2 Site Variational	8 State Simple Truncation	H 6	H 8	H 10
0	1	1	1	1	1	1	1
.4	.99491	.981175	.994946	.99175	.9949	.9949	.9949
.8	.97844	.932368	.979195	.9667	.9791	.979	.9792
1.	.96468	.898863	.966766	.94657	--	.9663	--
1.6	.88011	.759089	.905799	.83135	.8996	.8991	.9024
1.8	.81254	.695192	.87458	.74653	--	--	--
2.	0	.617524	.834992	0	.7991	.7798	.7483
2.2	0	.517748	.783132	0	.01876	--	~ 0
2.4	.370587	.710488	0	~ 0	~ 0	~ 0	~ 0
2.6	.006761	.589951	0	~ 0	~ 0	~ 0	~ 0
2.8	0	0	0	0	~ 0	~ 0	~ 0

Table III

GAP TO FIRST EXCITED STATE FOR SAME VALUES OF y FOR SAME SET OF CALCULATIONS

y	Exact Solution	2 Site Simple Truncation % Deviation	2 Site Variational	8 State Simple Truncation	H 6	H 8	H 10
0	0	0	0	0	0	0	0
2	0	0	0	.091255	0	0	0
2.2	.2	0	0	.279496	.080925	0	.186855
2.4	.4	0	0	.47269	.3879	--	.41901
2.8	.8	.39594	.21329	.865984	.8761	.7752	.846779
3.2	.889	.82186	1.291157	1.2857	1.19354	1.26033	
3.6	1.6	1.3427	1.30423	1.68605	1.6895	1.6039	1.665981
4	2	1.7793	1.75378	2.08235	2.0909	2.0108	2.06819

Table IV

$\frac{1}{V} \sum_{j} \langle \sigma_x(j)\sigma_x(j+1) \rangle$ FOR SAME VALUES OF y, CALCULATED BY THE SAME METHODS

y	Exact Solution	H 6	H 8	H 10
0	1	1	1	1
.8	.95872	.95949	.958572	.9596
1.6	.81256	.8856	.820244	.833924
2	.6366	.7285	.678385	.598118
2.2	.53032	.521475	.517788	.530175
2.8	.385996	.35997	.359447	.382808
3.2	.330596	.314026	.313516	.328424
4	.258656	.250674	.250323	.2575

Table V

$\frac{1}{V} \sum_{\partial} \langle \sigma_y(j)\sigma_y(j+1) \rangle$ FOR THE SAME VALUES OF y

y	Exact Solution	H 6	H 8	H 10
0	0	0	0	0
.8	.020866	.022308	.029666	.013988
1.6	.099213	.105604	.120316	.0605285
2	.21221	.193949	.22224	.138307
2.2	.27070	.339289	.329199	.264582
2.8	.27922	.307754	.306941	.280036
3.2	.26217	.280631	.279968	.262937
4	.22519	.234295	.233059	.2255

Table VI

$\frac{1}{V} \sum \langle \sigma_z(j)\sigma_z(j+1) \rangle$ FOR THE SAME VALUES OF y

y	Exact Solution	H 6	H 8	H 10
0	0	0	0	0
.8	.061728	.0628168	.071083	.053725
1.6	.27782	.27781	.29961	.224331
2	.54038	.487454	.539943	.428475
2	.68929	.800405	.792558	.693524
2.8	.84148	.023122	.920878	.853846
3.2	.44536	.944067	.94249	.895549
4	.93100	.965678	.964919	.9378

Table VII

VALUES OF THE CRITICAL POINT, CRITICAL EXPONENT FOR THE MAGNETIZATION AND SLOPE OF THE MASS GAP AT THE CRITICAL POINT, AS OBTAINED FROM THE VARIOUS CALCULATIONS. NOTE, THE DETERMINATION OF THE CRITICAL EXPONENT AND SLOPE IS FROM A FIT TO THE GRAPH AND IS ACCURATE TO ± .008

	Exact Solution	2 Site Simple Truncation	2 Site Variational	8 Site Example Truncation	H6	H8	H10
Critical Point	2	2.553	2.72	1.92	2.17	2.22	2.08
Critical Exponent	1/8	.38	.21	.13	.13	.14	.125
Slope of Gap Curve	1	1.151	1.276	1.00166	1.09945	1.0293	1.04166

FIGURE CAPTIONS

Fig. 1 The solid line is a graph of the exact ground state energy density of the theory as a function of $y = \varepsilon_0/\Delta_0$. The dotted line is the result of the two level variational renormalization group calculation. Note the results are better for $y < 2$ than for $y > 2$.

Fig. 2 The solid line is the exact ground state energy density as a function of $y = \varepsilon_0/\Delta_0$. The dotted line is the dual of the curve in Fig. 1 calculated for $y \leq 2$. Note the improvement in behavior for large y.

Fig. 3 The solid line is the exact ground state energy density, the points are the results of the ten state hybrid calculation .

Fig. 4 The solid curve is the exact analytic form of the magnetization, $\langle\sigma_x\rangle = \frac{1}{V}\sum_{\sigma}\langle\sigma_x(j)\rangle$, plotted as a function of $(y/y_c = 2.08)$ instead of $(y/2)$. The circles are the results of a point by point hybrid calculation.

Fig. 5 The solid curve is the analytic form of the second derivative of the groundstate energy density as a function of y plotted for $y_c = 2.08$ instead of the exact value $y_c = 2$. The circles are results of the hybrid calculation.

Fig. 6 The solid curve is the exact nearest neighbor correlation function $\frac{1}{V}\sum \langle(\sigma_x)j)\ \sigma_x(j+1)\rangle$ (i.e., $y_c = 2$), the circles are results of the hybrid calculation.

Fig. 7 The solid curve is the exact value of $\frac{1}{V}\sum_{j}\langle\sigma_y(j)\sigma_y(j+1)\rangle$ versus $y^2\varepsilon_o/\Delta_o$. Open circles are the results of the 10 state hybrid calculation.

Fig. 8 The solid curve is the exact form of $\frac{1}{V}\sum_{\partial}\langle\sigma_z(j)\sigma_z(j+1)\rangle$, open circles are the results of the 10-state hybrid calculation.

Fig. 9 The solid curve is the exact value of the mass gap to the first excited state as a function of $y = \varepsilon_o/\Delta_o$ for $y \geq z$. Open circles are the results of our approximate calculation.

Fig. 10 A comparison of several different hybrid calculations for the ground state energy density with the exact answer.

Fig. 11 A comparison of two different calculations of the mass gap with the exact solution.

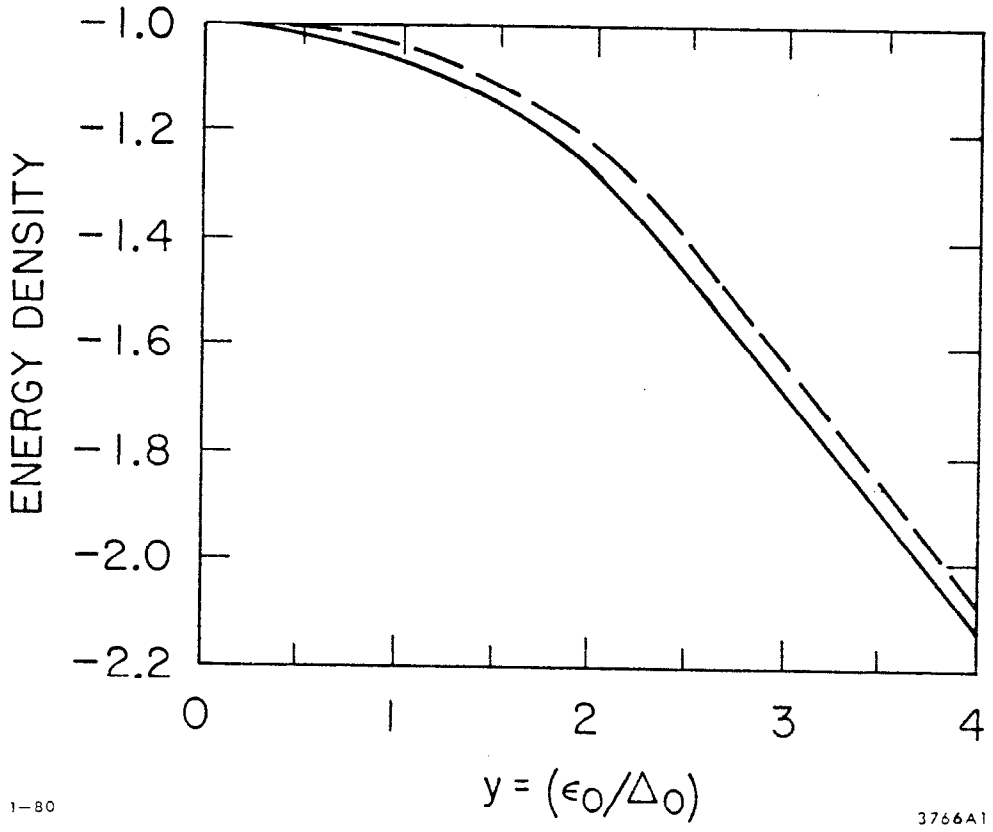

Fig. 1

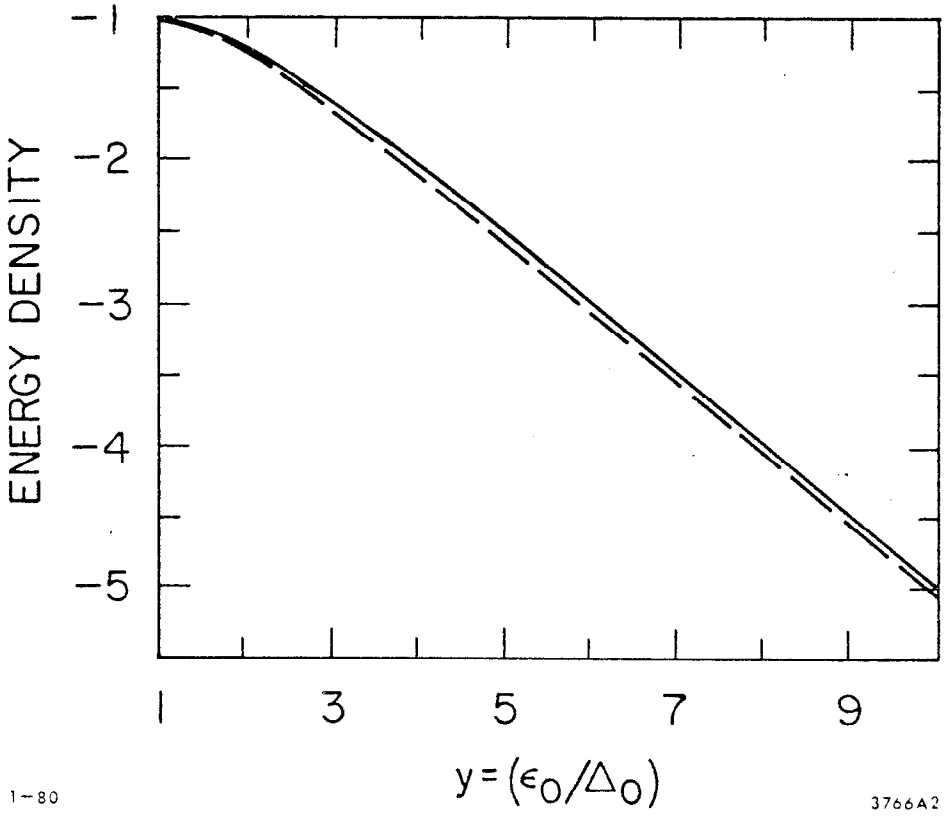

Fig. 2

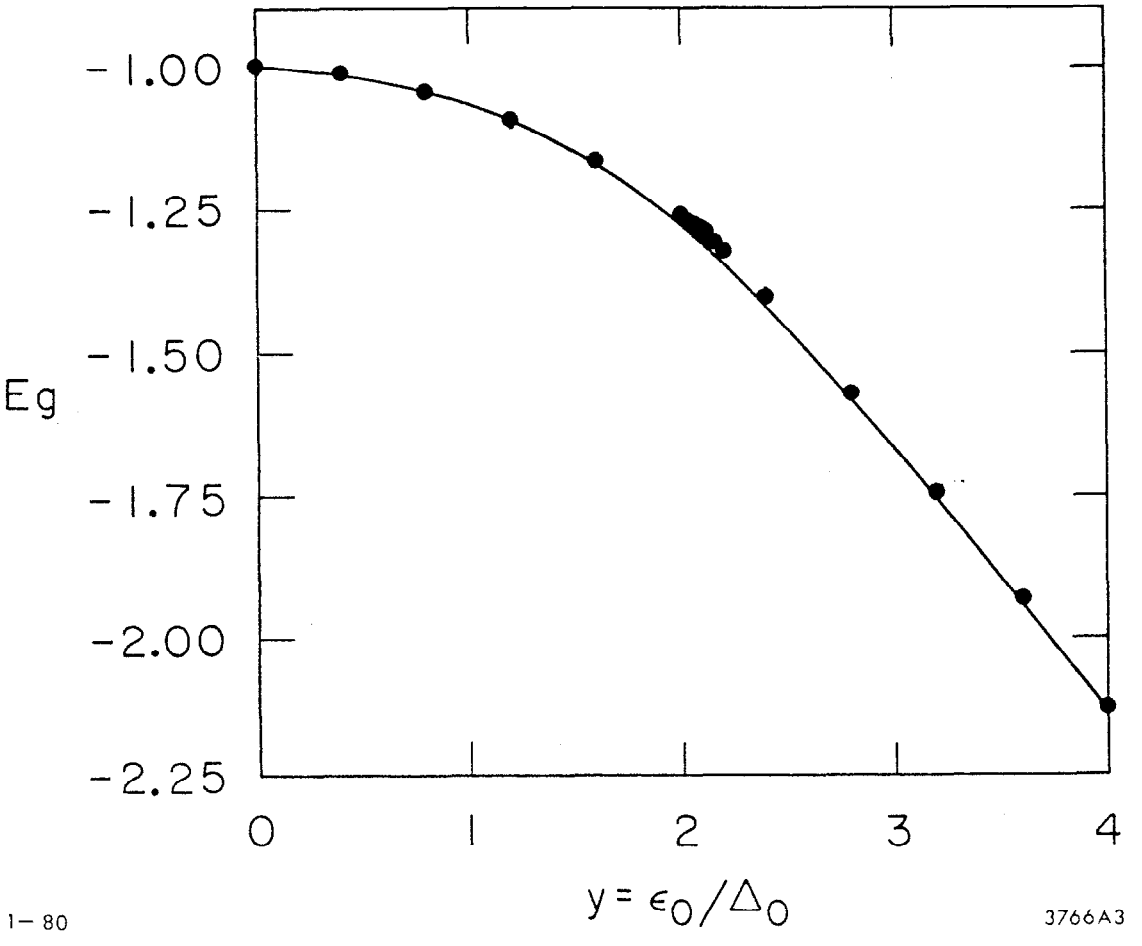

Fig. 3

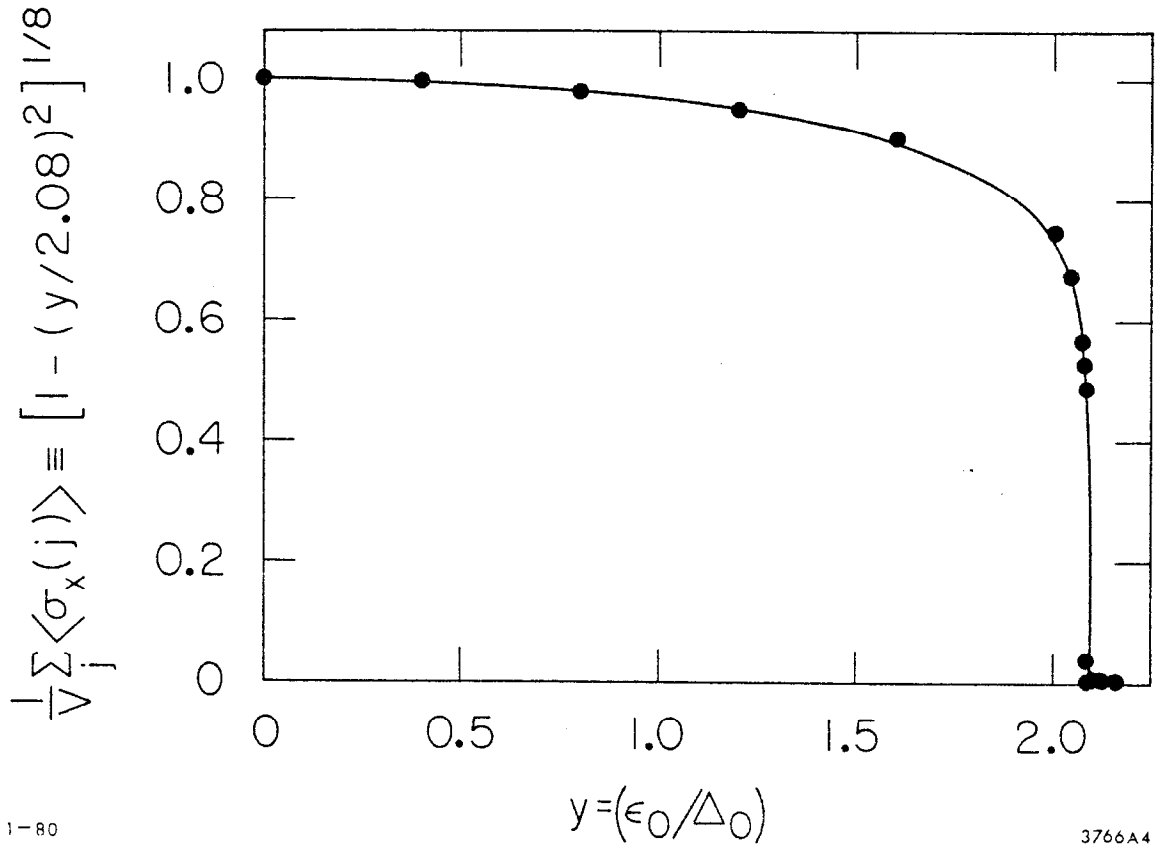
$\frac{1}{V}\sum_{i,j}\langle\sigma_x(ij)\rangle \equiv \left[1-(y/2.08)^2\right]^{1/8}$
1.0
0.8
0.6
0.4
0.2
0
0
0.5
1.0
1.5
2.0
$y=(\epsilon_0/\Delta_0)$
1-80
3766A4

Fig. 4

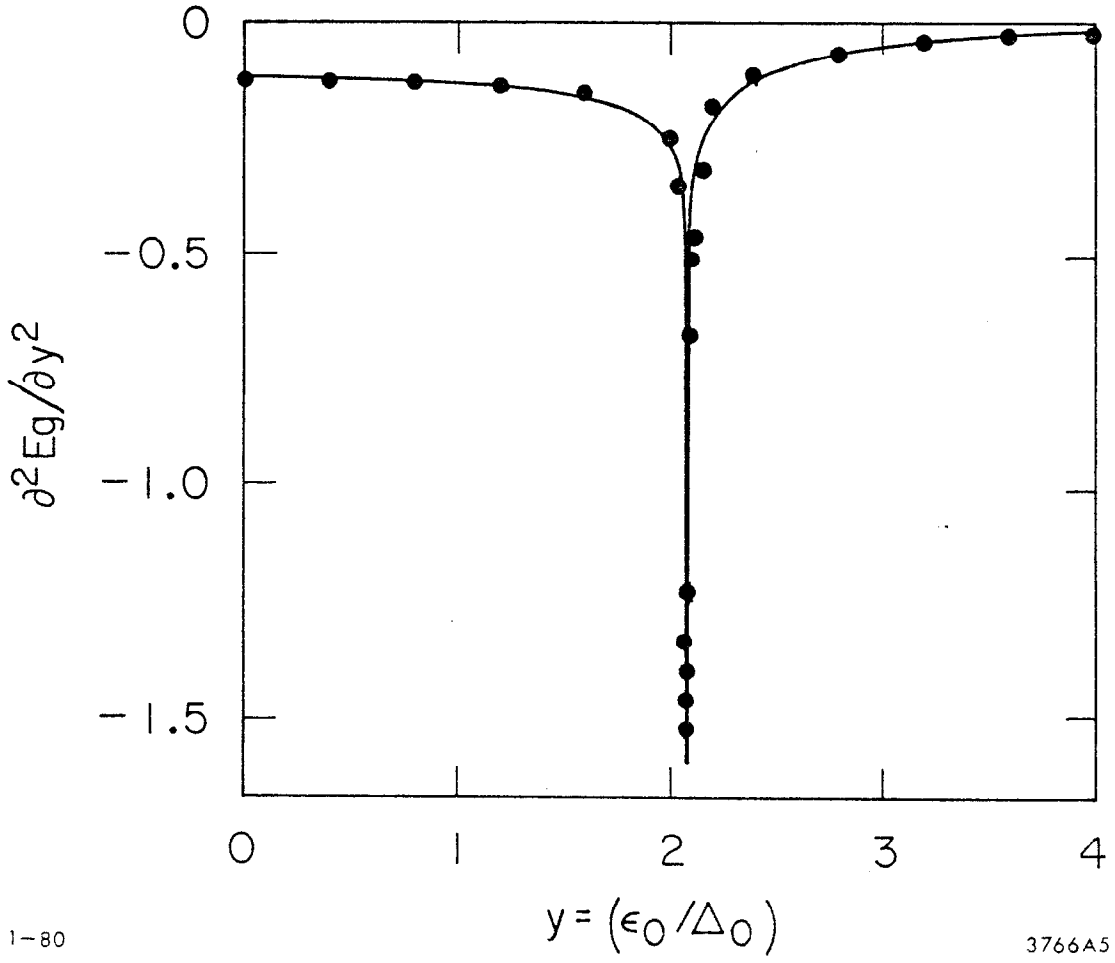
0
−0.5
−1.0
−1.5
$\partial^2 Eg/\partial y^2$
0
1
2
3
4
$y = (\epsilon_0/\Delta_0)$
1−80
3766A5

Fig. 5

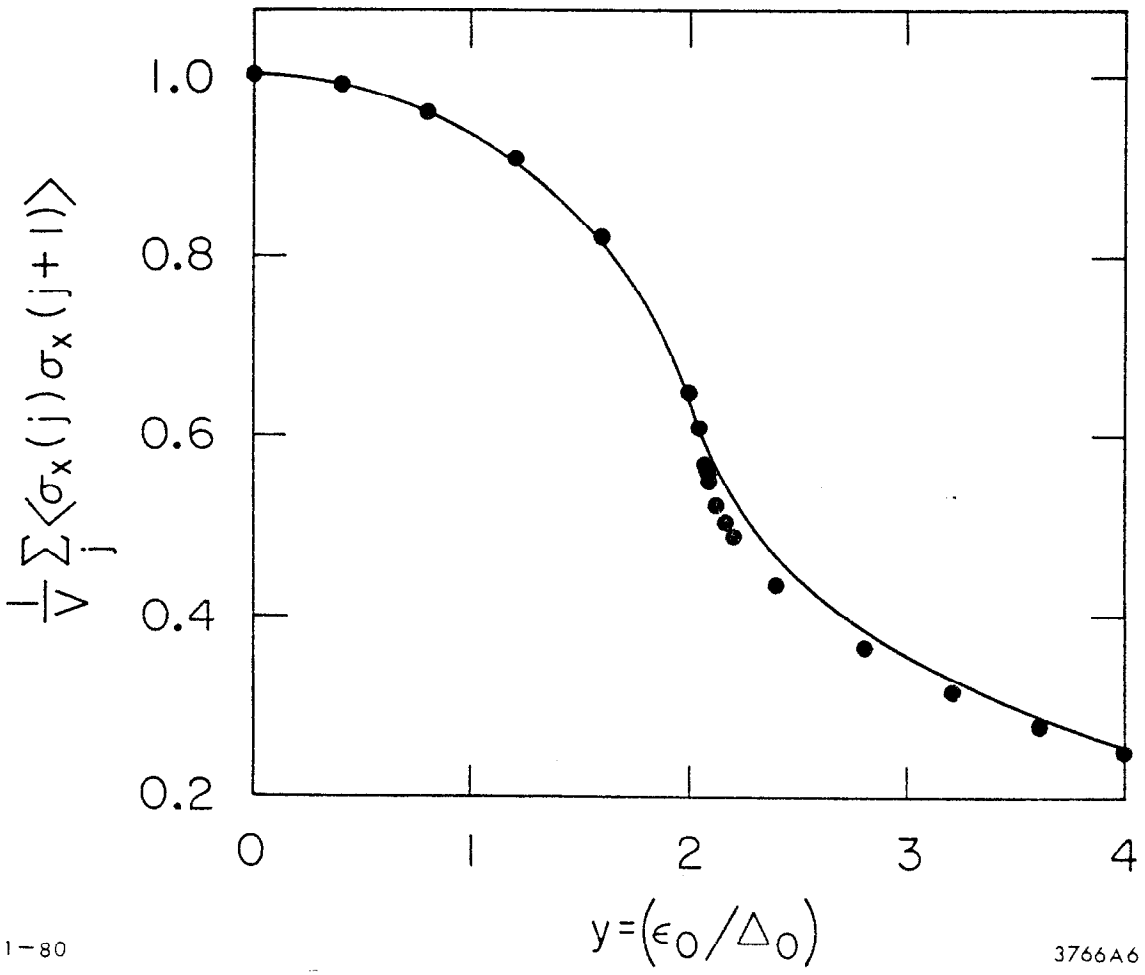
1.0
0.8
0.6
0.4
0.2
0
1
2
3
4
$\frac{1}{N}\sum_j \langle \sigma_x(j)\sigma_x(j+1)\rangle$
$y=(\epsilon_0/\Delta_0)$
1-80
3766A6

Fig. 6

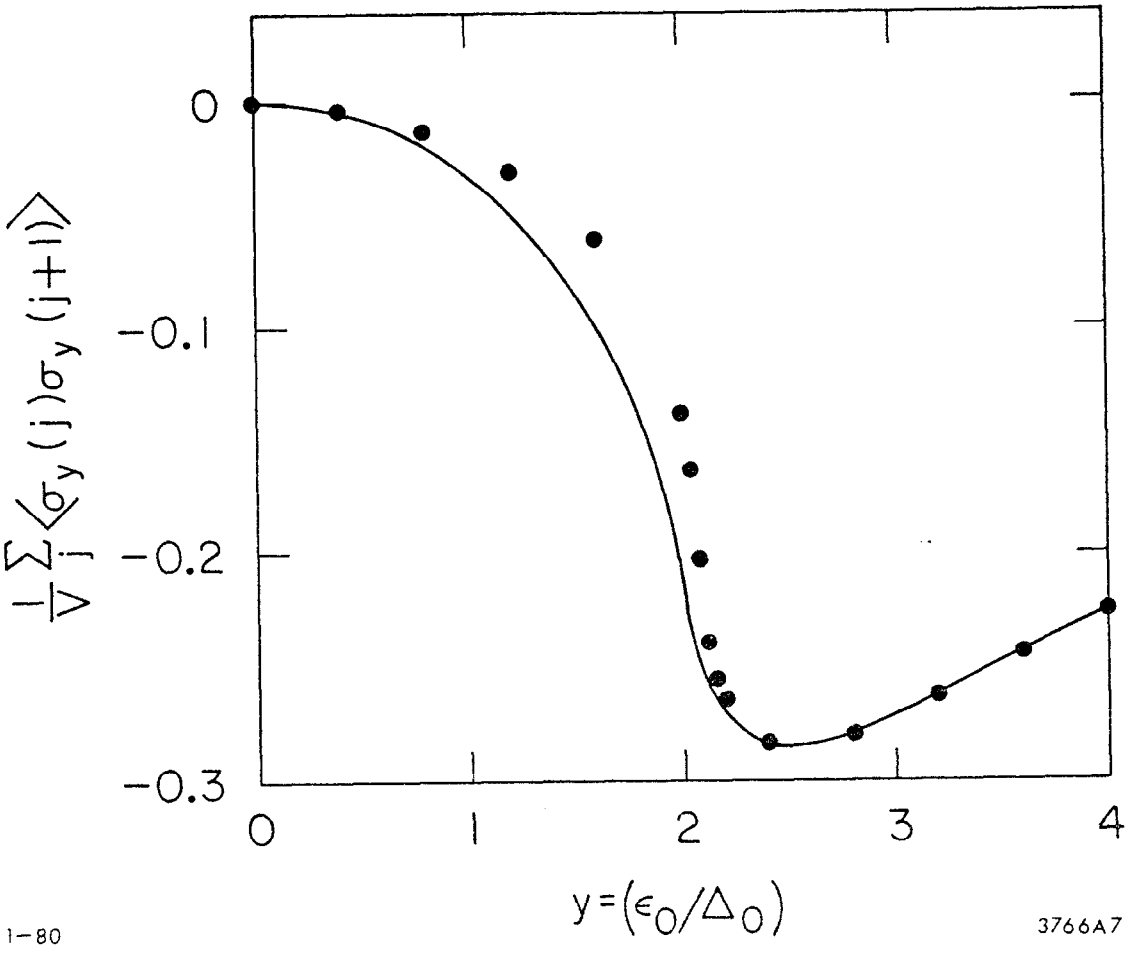
0
-0.1
-0.2
-0.3
0
1
2
3
4
$\frac{1}{N}\sum_j \langle \sigma_y(j)\sigma_y(j+1)\rangle$
$y=(\epsilon_0/\Delta_0)$
1-80
3766A7

Fig. 7

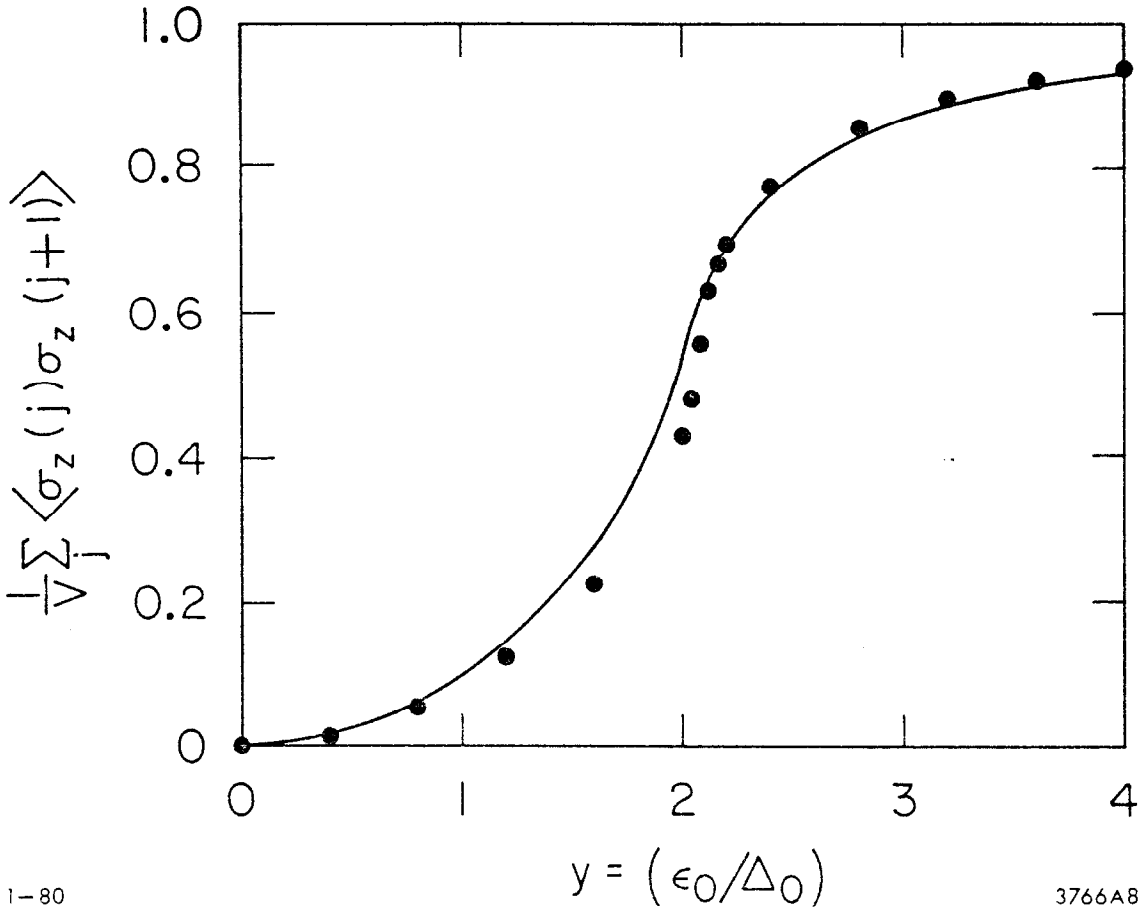
1.0
0.8
0.6
0.4
0.2
0
0
1
2
3
4
$\frac{1}{V}\sum_{j}\langle\sigma_z(j)\sigma_z(j+1)\rangle$
$y = (\epsilon_0/\Delta_0)$
1-80
3766A8

Fig. 8

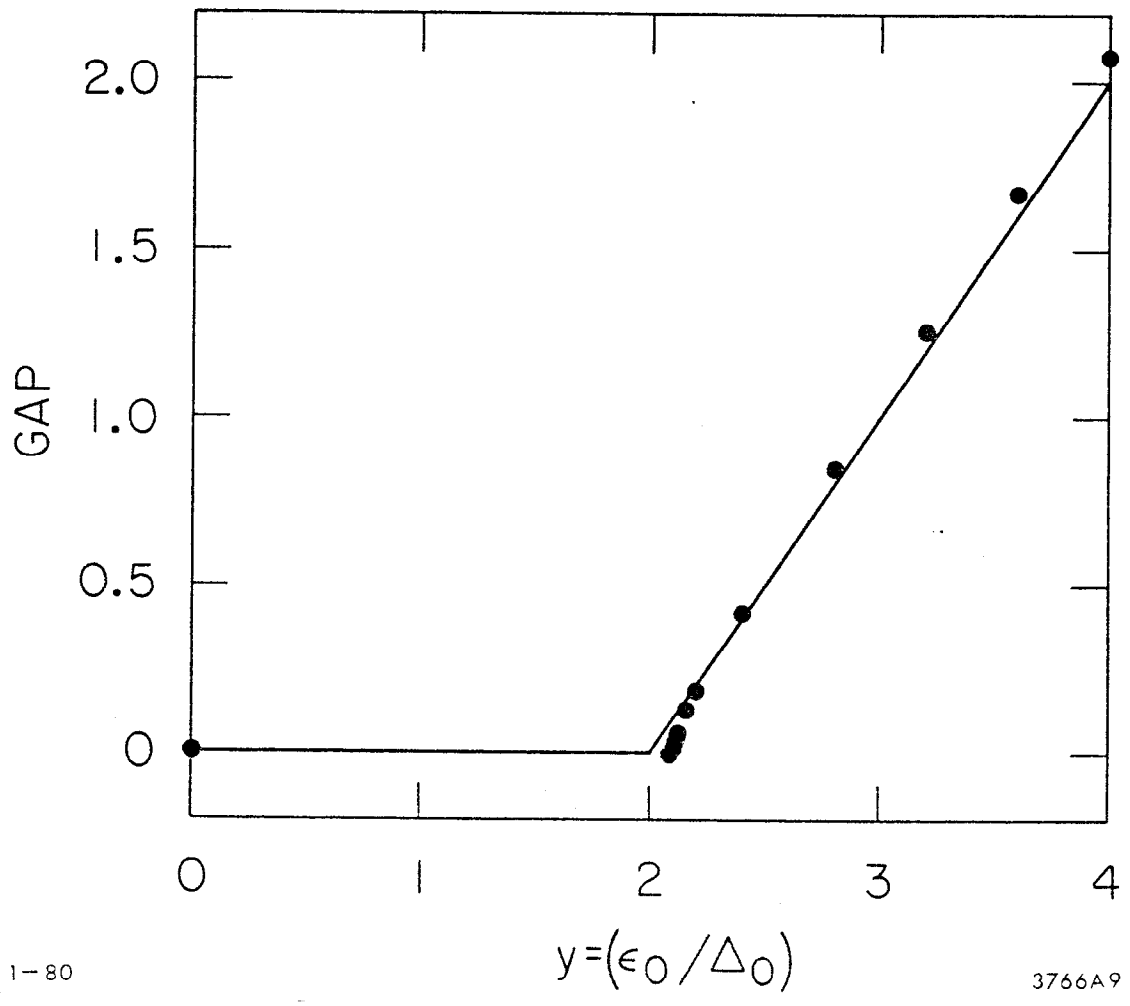

Fig. 9

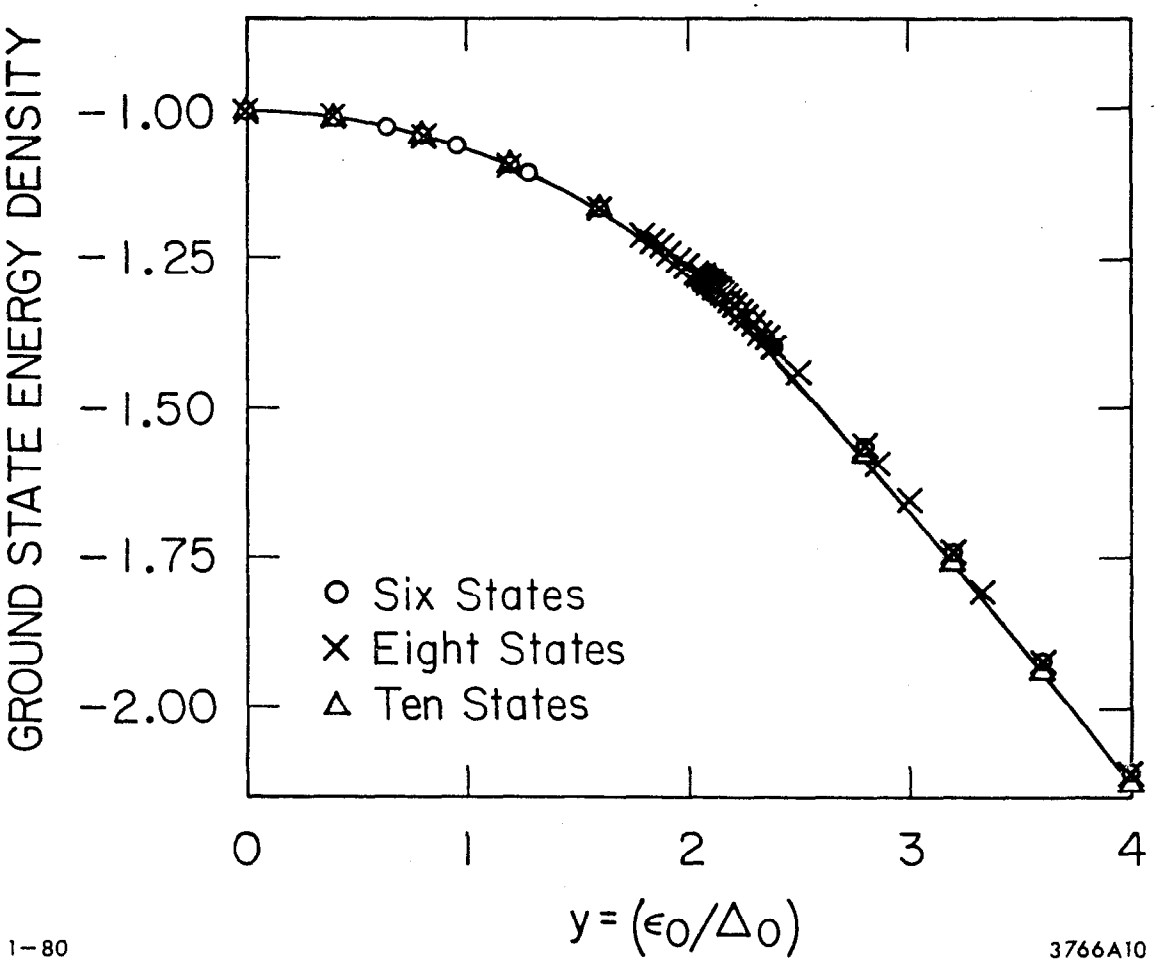
GROUND STATE ENERGY DENSITY
-1.00
-1.25
-1.50
-1.75
-2.00
0
1
2
3
4
y = (ε0/Δ0)
o Six States
× Eight States
△ Ten States
1-80
3766A10

Fig. 10

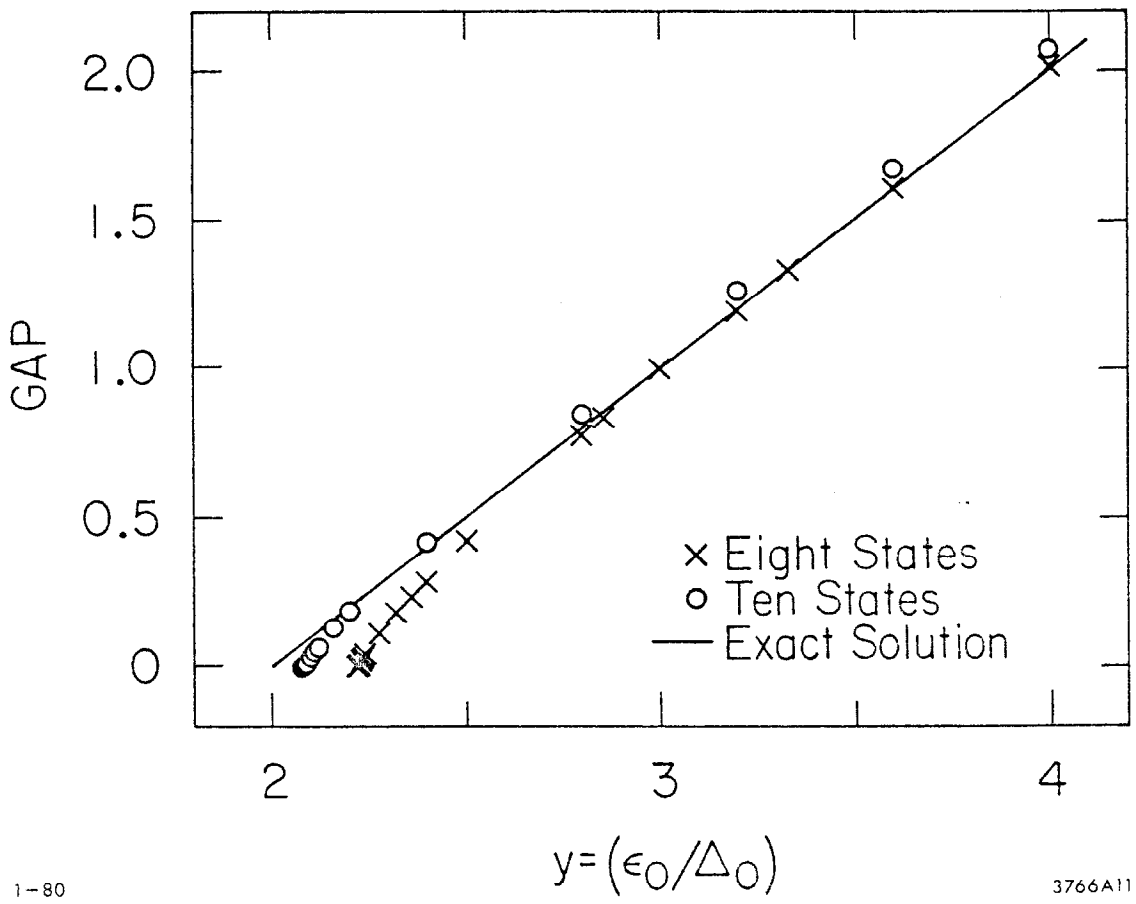
2.0
1.5
1.0
0.5
0
GAP
2
3
4
y=(ϵ0/Δ0)
× Eight States
o Ten States
— Exact Solution
1-80
3766A11

Fig. 11